www.czasopisma.pan.pl PAN www.journals.pan.pl

Metrol. Meas. Syst., Vol. XXI (2014), No. 3, pp. 423–432.

PAN POLSKA AKADEMIA NAUK

METROLOGY AND MEASUREMENT SYSTEMS

Index 330930, ISSN 0860-8229

www.metrology.pg.gda.pl

M&MS

INFLUENCE OF A/D QUANTIZATION IN AN INTERPOLATED DFT BASED SYSTEM OF POWER CONTROL WITH A SMALL DELAY

Józef Borkowski, Dariusz Kania, Janusz Mroczka

Chair of Electronic and Photonic Metrology, Wroclaw University of Technology, B. Prusa 53/55, 50-317 Wroclaw, Poland (Jozef.Borkowski@pwr.edu.pl; ✉ Dariusz.Kania@pwr.edu.pl, +48 508 632 287; Janusz.Mroczka@pwr.edu.pl)

Abstract

Fast and accurate grid signal frequency estimation is a very important issue in the control of renewable energy systems. Important factors that influence the estimation accuracy include the A/D converter parameters in the inverter control system. This paper presents the influence of the number of A/D converter bits b, the phase shift of the grid signal relative to the time window, the width of the time window relative to the grid signal period (expressed as a cycle in range (CiR) parameter) and the number of N samples obtained in this window with the A/D converter on the developed estimation method results. An increase in the number b by 8 decreases the estimation error by approximately 256 times. The largest estimation error occurs when the signal module maximum is in the time window center (for small values of CiR) or when the signal value is zero in the time window center (for large values of CiR). In practical applications, the dominant component of the frequency estimation error is the error caused by the quantization noise, and its range is from approximately 8×10^{-10} to 6×10^{-4}.

Keywords: photovoltaic system, frequency estimation, signal processing, A/D converter, control of power system.

1. Introduction

It is difficult to imagine our life without electricity. In recent years, renewable energy sources have become very popular around the world because of their high availability, "clean energy" production and ability for individuals to install their own systems [1]. The main reason for the popularity of these energy sources is because traditional energy sources will end one day and will have to be replaced.

Among the sources of renewable energy, solar energy is one of the most commonly used. Photovoltaic systems used for the solar energy conversion into electricity are constantly improved in the hardware and software [2–3]. One of the basic elements of the photovoltaic system is an inverter that is used to convert DC current and voltage obtained from photovoltaic cells to AC current and voltage with specified parameters. The energy produced by renewable energy systems (as well as the safety of the production) must fulfill the requirements defined in the respective standards and directives, such as IEC 61727-2002, IEEE Std 929-2000 and others [4–6].

One of the key issues for electricity production in photovoltaic systems is the grid signal parameters' estimation. This allows the proper control of the inverter and improvements in the quality of the produced energy [7–9]. The main estimated parameter is grid signal frequency. There are several methods for the sinusoidal signal frequency estimation. These can be divided into spectral methods of analysis and other methods e.g., the Prony method, the transmission modeling method, and subspace methods [10–12]. The methods of the first

Article history: received on Jun 05, 2014; accepted on Jul. 04, 2014; available online on Sep. 15, 2014; DOI: 10.2478/mms-2014-0036.

group are less accurate but fast, and the methods of the second group are more accurate but more computationally expensive. A method that allows very fast and accurate frequency estimation is proposed in [13] (the principle of operation is briefly discussed in Section 2).

The quality of the estimation is dependent not only on the method but also on the hardware. The poor A/D converter quality in the control system unit can result in a significant loss of the produced energy quality [14–16]. This paper presents the information necessary to determine the number of A/D converter bits for a given number of samples and width of the time window so that the estimation error of the method of [13] is at a certain level.

The remainder of this paper is organized as follows. In Section 2, the principle of operation for the frequency estimation method is presented. Section 3 contains a simulation study for the influence of the sliding time window's phase on the frequency estimation error. Section 4 presents the results of research for the worst sliding window's phase cases. Section 5 contains information on how to choose the number of A/D converter bits so that the estimation error is at certain level of accuracy. Finally, the conclusions are presented in Section 6.

2. The continuous tracking system with low delay

The fast, accurate and permanent (continuous tracking) parameters estimation of the grid signal is described in the time domain as:

$$x(t) = \sum_{i=1}^{M} A_i \sin(2\pi f_i t + \varphi_i), \tag{1}$$

i.e., the sum of a finite number of sinusoidal oscillations, each of which is characterized by the amplitude A_i, frequency f_i and phase angle φ_i and is necessary for proper signal generation in the system of power control.

The fundamental frequency (for i=1) is the most distorted in a deterministic manner (e.g., harmonics and interharmonics of the signal (for i=1)) or a random manner (e.g., white noise, "colored", quantization noise caused by the A/D converter) (Fig. 1a). After sampling, the $x(t)$ signal with a frequency f_s=1/T N samples x_n=x(nT), where n=0,…,N-1 are obtained.

Currently, renewable energy systems are often used to produce electricity, e.g., photovoltaic systems. A basic diagram of a photovoltaic system consisting of solar panels, inverter and control unit is shown in Fig. 1a. The DC signal obtained from the solar panels must be converted in a specific way to the AC signal using the inverter. There are several structures of inverter control units. Most of them are based on the grid signal parameter values obtained from the feedback [17–19]. Thus, the control algorithm adjusts the control signals (e.g., the frequency of the switching transistors in the inverter) so that the signal produced at the system output fulfills the quality standards [20–22].

One of the most important blocks in the control system is the DSP unit, which is responsible for the estimation of the grid signal parameters, such as f_1, A_1, φ_1, THD, and Q (Fig. 1b). The value of the signal frequency f_1 is used, e.g., in under/over frequency protection algorithms or in resonant controllers to shape the appropriate response characteristics [23]. The value of the signal amplitude A_1 is used e.g., in under/over voltage protection algorithms [24]. The value of the phase angle φ_1 is mainly used to synchronize the voltage and current at the system output and in islanding protection algorithms [25]. For the accuracy of the entire system, it is essential to accurately estimate the frequency f_1 because most often, on this basis other parameters can be determined.

In [13], the method for calculating the grid signal frequency estimation in photovoltaic systems is presented, although it can be successfully applied in other renewable systems (and not only there). The method allows to determine the normalized grid signal frequency λ_1=f_1T_0

Metrol. Meas. Syst., Vol. XXI (2014), No. 3, pp. 423–432.

(where the width of the sliding time window T_0 expressed in the time unit is $T_0=NT$) by considering the impact of the conjugate component. The unit of λ is Hz/Hz, which is marked as a bin, and λ is referred to as cycle in range (*CiR*). The method uses the maximum decay sidelobes windows (for the window order H=2) and three relevant consecutive points of the spectrum $X(\lambda)$ for $\lambda = k–1, k, k+1$ (values $X_{k–1}$, X_k, X_{k+1}) around the main lobe. Developing the method for H>1, the frequency estimation is performed on the basis of:

$$\Pi_1 - \lambda_1^2 \Pi_2 = 0\,, \tag{2}$$

where

$$\Pi_1 = \begin{vmatrix} (2H-1)H & (2H-1) & X_{k-1} - X_k \\ -k^2 - H^2 & 2k & X_k \\ (2H-1)H & -(2H-1) & X_{k+1} - X_k \end{vmatrix}, \tag{3}$$

$$\Pi_2 = \begin{vmatrix} 1 & -(2H-1) & X_{k-1} \\ 1 & 0 & X_k \\ 1 & (2H-1) & X_{k+1} \end{vmatrix}. \tag{4}$$

The accuracy of the frequency estimation is on the order of $5\cdot10^{-11}$ Hz/Hz for a 5-ms measurement window. In comparison, the relative errors of the other spectral methods are approximately 10^{-7} Hz/Hz. The possibility of using different windows from the discussed family has several advantages – it is possible to match the specific window data to the actual requirements of electricity generation. In addition, the discussed estimation method applies to one sinusoid, but it can be generalized to a multi-frequency signal.

The accuracy of the f_1 estimation is influenced by (Fig. 1a): the *CiR* width of the time window (relative to the period $T_1=1/f_1$), the signal phase angle φ_1 relative to the beginning of

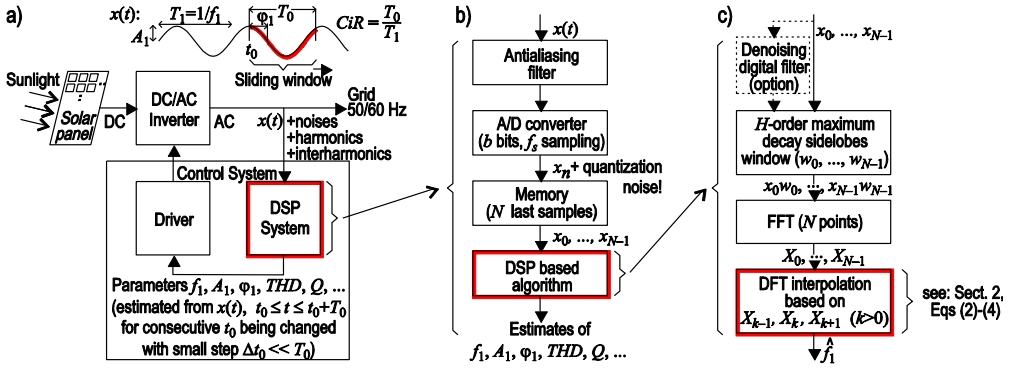

Fig. 1. The real-time inverter control unit in the photovoltaic system with a sliding time window: a) the general system scheme with the definition of the sliding window *CiR* width and the *x(t)* signal angle phase φ_1 relative to the window beginning (or equivalently the angle phase $\varphi_1 + 0.5CiR\times2\pi$ relative to the window center); b) the DSP block diagram of the control unit along with the selected influence of the A/D converter quantization noise with a sampling frequency f_s; c) the algorithm to estimate the fundamental frequency f_1 of the grid signal *x(t)*.

the time window (or equivalently the phase $\varphi_1 + 0.5CiR \times 2\pi$ [rad] of the signal relative to the center of the time window) and signal interferences, which may be deterministic disturbances or random noise.

The aim of this study is to answer the question of how quantization (caused by using the A/D converter) influences the estimation accuracy and how to optimally select the number of the A/D converter bits b (Fig. 1b) using the discussed method (Fig. 1c). Therefore, it is assumed in further analysis that the quantization noise of the A/D converter is the dominant source of signal interferences. It is also worth noting that the low-pass filter or band-stop filter that is visible in Fig. 1c (the denoising digital filter) can remove a number of signal interferences that influence the accuracy of the f_1 estimation, but it has no effect on the level of quantization noise brought by the A/D converter. The selection of the number of bits b depends on the parameter CiR and φ_1 (equivalently $\varphi_1 + 0.5CiR \times 2\pi$), and it must take into account the following limitations:

– the value of CiR cannot be in practice greater than the maximum trip time defined in the standards (Tab. 1), which means that the CiR value should not exceed the 2-2.5 value (50-33.3 ms); in practice, the CiR value should be smaller to shorten the response time of the system for the appearance of system operation irregularities, but the smaller the CiR value is, the greater the influence of the interferences (including quantization noise) is on the f_1 estimation accuracy and other parameters.

– the angle phase φ_1 (or $\varphi_1 + 0.5CiR \times 2\pi$) in the continuous tracking system of the AC signal parameters changes its value in the full range (from 0 to 2π rad), and how the angle phase influences the f_1 estimation accuracy should be determined. In particular, the least favorable cases should be determined for the estimation accuracy.

In the case of the multi-frequency signal (which occurs in the grid), proper filtration is important before the estimation (denoising digital filter in Fig. 1c). Because of the limited trip times, the filtration must also be conducted very fast to maintain a good performance.

Tab. 1. Maximum trip times for voltage, amplitude and frequency according to the standards IEEE 929-2000 and IEC 61727-2002.

IEEE 929-2000		**IEC 61727-2002**	
Voltage range [%]	**Maximum trip time [s]**	**Voltage range [%]**	**Maximum trip time [s]**
V < 50	0.100	V < 50	0.100
50 ≤ V < 88	2.000	50 ≤ V < 85	2.000
110 < V < 137	2.000	110 < V < 135	2.000
V ≥ 137	0.033	V ≥ 135	0.050
Frequency range [Hz]	**Maximum trip time [s]**	**Frequency range [Hz]**	**Maximum trip time [s]**
59.3 > f > 60.5	0.100	49 > f >51	0.200
Normal operation: 88 % (105.6 rms) ≤ V ≤ 110 % (132 rms) and 59.3 Hz ≤ f ≤ 60.5 Hz		**Normal operation:** 85 % (195.5 rms) ≤ V ≤ 110 % (253 rms) and 49 Hz ≤ f ≤ 51 Hz	

3. Influence of the sliding time window's phase

The photovoltaic system in Fig. 1 operates in real time and in continuous mode, i.e., the sliding of the time window is performed with a small step. The last N samples of the signal are stored in the DSP memory because they are needed to calculate the current frequency estimate. The frequency value is updated every 4 sampling periods (167 μs) [13]. The high influence on the systematic error δf_1 has φ_1 and CiR (but also b, N, k and H). This dependence can be reduced to a value equal to $\varphi_1 + 0.5CiR \times 2\pi$ [rad], which is the signal angle phase relative to the sliding window center and not the sliding window's beginning.

Metrol. Meas. Syst., Vol. XXI (2014), No. 3, pp. 423–432.

The systematic error plot depends on the signal phase shift (without quantization) and has local maxima relative to the sliding window center: one smaller for $m\pi+\pi/2$ (m – integer) and one larger – the global maximum – for $m\pi$ (Fig. 2a). For integer CiR values (1 or 2), the systematic error is equal to 0 (in practice the error is non-zero because of the finite arithmetic precision used). The maximum of the systematic error calculated for $\varphi_1=0,...,2\pi$ at a given CiR value is inversely proportional to N^4 (Fig. 2b). The minimum of the systematic error can be obtained for $k = 1$ for $CiR < 2.08$ and $k = 2$ for $CiR \geq 2.08$. Increasing the number of samples at the constant CiR value reduces this error. Analogous to the Cramer-Rao bound behavior for the frequency estimator, the systematic error significantly increases when the CiR value is smaller than ca. 0.8 bin.

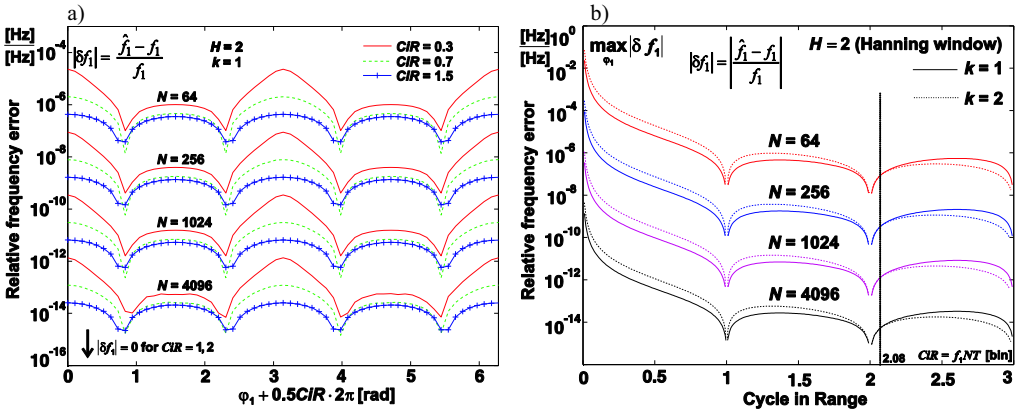

Fig. 2. The systematic error δf_1 of the f_1 estimation for the method from [13] without quantization and various N: a) dependence on the signal phase shift and its position relative to the time window center; b) the maximum systematic error calculated for $\varphi_1=0,...,2\pi$.

It is necessary to use the A/D converter to convert the analog signal to a digital signal. Unfortunately, in the process, undesirable quantization noise is present, and it is the greater than the smaller number of A/D converter bits b (the number of bits on which the conversion result is stored in the U2 code).

Computer simulations were performed in the Matlab environment, and they include the study of the influence of N, CiR and $\varphi_1 +0.5CiR\times2\pi$ on the grid signal frequency estimation in two cases: 1) the A/D converter with an infinite number of bits was used (no quantization, the number of bits $b\rightarrow\infty$) and 2) the A/D converter with a finite number of bits $b \geq 8$ was used.

The accuracy of the estimation is affected by the grid signal phase shift relative to the time window, and the position of the estimation error maxima is fixed relative to the time window center i.e., the phase $\varphi_1 +0.5CiR\times2\pi$ (Fig. 2a). For small values of CiR (less than 1), the largest estimation error occurs when the signal value is zero in the time window center (case $\varphi_1 +0.5CiR\times2\pi = 0, \pi, 2\pi, ...$). For larger values of CiR (above 1), the situation is reversed (Fig. 3). The accuracy of the estimation is also affected by the number of A/D converter bits b, the value of CiR and the number of samples N (Fig. 3). The estimation error decreases when the values of these parameters increase. The choice of b is of particular importance. An increase in the number of bits by 8 causes a decrease in the estimation error of approximately $2^8=256$ times. The signal of the systematic error is periodic. Its shape is associated with the measurement window shifting and the grid signal periodicity.

Further studies describe the accuracy analysis of the frequency estimation method for the largest error case in the entire range of the grid signal phase shift for given b, CiR, k and H

parameters. It is the worst estimation accuracy case, and it is the most interesting case for practical applications of this method.

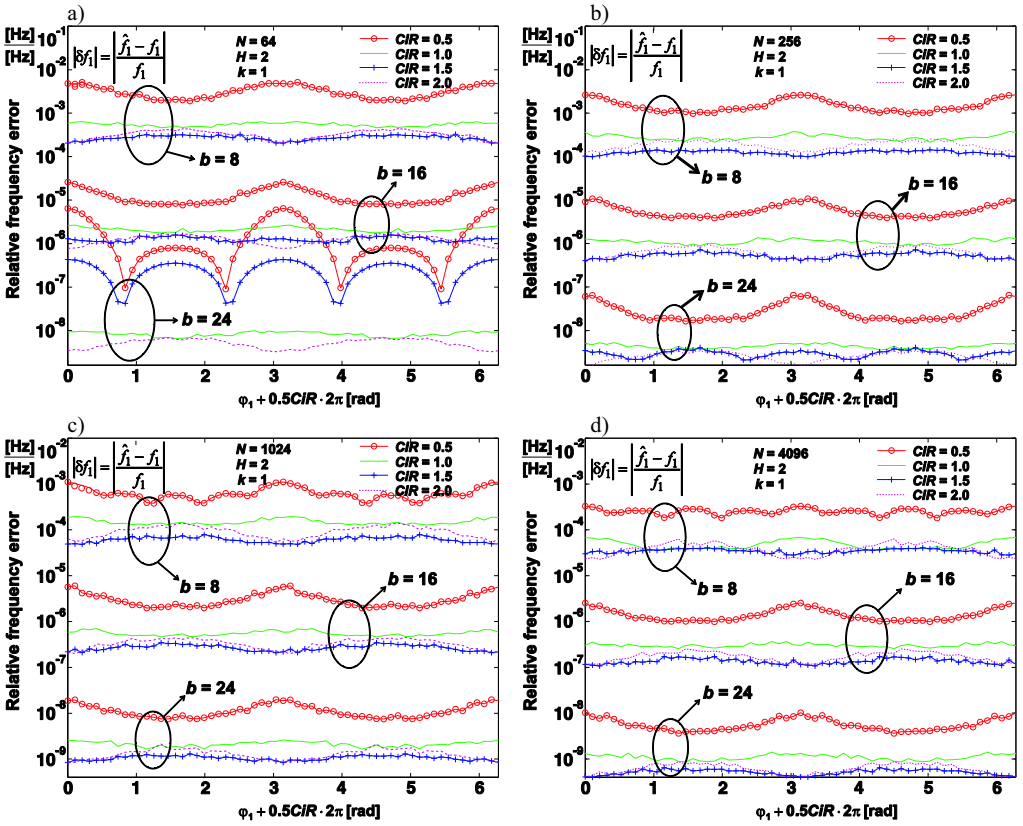

Fig. 3. The influence of the number of A/D converter bits b on the relative frequency error for:
a) N=64; b) N=256; c) N=1024; d) N=4096.

4. The worst sliding window phase case

From a practical point of view, the most interesting case is the case of the worst estimation error depending on the grid signal phase (the maximum estimation error that may occur using the discussed method). The maximum level of the estimation error for the given H value depends on the number of A/D converter bits b and the CiR value, N value and k value (Fig. 4). The curves in Fig. 4 have a number of local maxima and minima because of the random nature of the errors caused by the quantization noise. It applies to those cases for which the dominant element is the error caused by the quantization noise, e.g., for b=8.

Metrol. Meas. Syst., Vol. XXI (2014), No. 3, pp. 423–432.

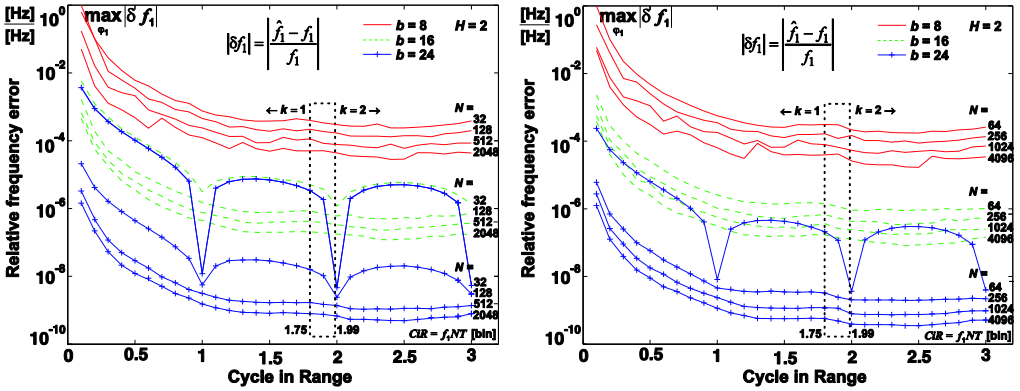

Fig. 4. The relative error δf_1 of the f_1 estimation for the method from [13] with quantization and: a) N=32, 128, 512, and 2048; b) N=64, 256, 1024, and 4096. The maximum systematic error calculated for φ_1=0,...,2π.

The quantization of the grid signal causes the k value to shift from 1 to 2, for which the estimation error is the smallest (without quantization, this value for H=2 is 2.08). Errors due to quantization reduce this level. For N=32,…,4096 and b=8,…,30, the threshold value varies in the range from 1.75 to 1.99 (Tab. 2). The higher the b value, the smaller the effect of quantization on the threshold. This means that the influence of the systematic error on the estimation accuracy increases, while the influence of the error due to quantization decreases. For the practical use of the method (for $N \geq 128$ and b= 8,…,24), it can be assumed that the threshold value is 1.8.

Tab. 2. Recommended *CiR* thresholds for the change k from 1 to 2 depending on N and b.

N	b											
	8	10	12	14	16	18	20	22	24	26	28	30
32	1.76	1.76	1.77	1.82	1.88	1.95	1.98	1.99	1.99	1.99	1.99	1.99
64	1.76	1.76	1.76	1.77	1.83	1.84	1.90	1.96	1.99	1.99	1.99	1.99
128	1.76	1.76	1.76	1.77	1.82	1.82	1.82	1.85	1.92	1.97	1.99	1.99
256	1.76	1.76	1.76	1.77	1.81	1.81	1.81	1.81	1.81	1.90	1.93	1.97
512	1.76	1.76	1.76	1.76	1.79	1.81	1.81	1.81	1.81	1.81	1.82	1.87
1024	1.75	1.75	1.75	1.75	1.79	1.79	1.79	1.79	1.79	1.80	1.80	1.81
2048	1.75	1.75	1.75	1.75	1.79	1.79	1.79	1.79	1.79	1.80	1.80	1.81
4096	1.75	1.75	1.75	1.75	1.76	1.77	1.77	1.77	1.78	1.80	1.80	1.80

5. Choose the number of bits for the A/D converter

The main aim of this paper is to show the influence of the number of A/D converter bits b in the system in Fig. 1 on the accuracy of the grid signal frequency estimation using the method from [13]. The estimation result is also influenced by the previously defined N, *CiR*, H and k parameters. If the values of these parameters are known, the value of b can be set so that the estimation error is at a specific level. It is important from a practical point of view where to begin the experiment the A/D converter should be used with a specified number of bits.

Theoretically, the b value can be chosen so that the error caused by the grid signal quantization was comparable to the systematic error (for $b \to \infty$). Therefore, the total error (shown in Fig. 5a as a red dashed line) would be no greater than twice the systematic error (Fig. 5a). This means the choice of b determines whether the quantization maintains the total error at approximately the systematic error level. In practical applications, where N is e.g.,

512, the error caused by the use of conventional A/D converters (8-24 bits) is several times greater than the systematic error (Fig. 5b). Theoretically, the N value can be decreased, but because of other factors, the value should be sufficiently large.

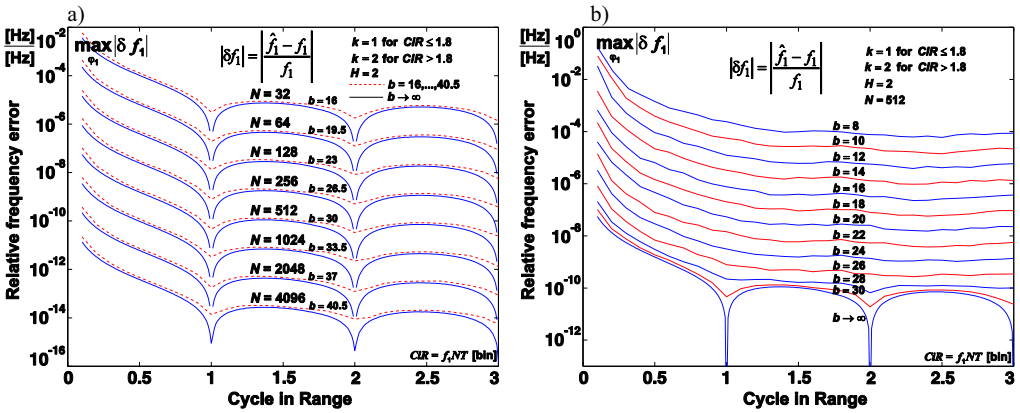

Fig. 5. The relative error δf_1 of the f_1 estimation for the method from [13] with quantization and: a) various N and b, which maintain the quantization error at approximately the systematic error level; b) various b and N=512.

The total error $|\delta f_1|$ is the sum of two components: the systematic error component $|\delta_s f_1|$ (with the ideal sampling, $b \to \infty$) and the component $|\delta_b f_1|$ caused by the quantization noise by using the A/D converter with a finite number of bits b:

$$\max_{\varphi_1}|\delta f_1| = \max_{\varphi_1}|\delta_s f_1| + \max_{\varphi_1}|\delta_b f_1|, \tag{5}$$

where the rough upper limits of both components of the total error can be estimated using the following equations (Fig. 6):

$$\max_{\varphi_1}|\delta_s f_1| \le \begin{cases} \dfrac{40}{N^4 CiR^2} & \text{for} \quad CiR < 0.5 \\ \dfrac{10}{N^4 CiR^4} & \text{for} \quad 0.5 \le CiR \le 1, \\ \dfrac{10}{N^4 CiR^{0.8}} & \text{for} \quad CiR \ge 1 \end{cases} \tag{6}$$

$$\max_{\varphi_1}|\delta_b f_1| \le \begin{cases} \dfrac{1.5}{2^b\sqrt{N}}\dfrac{1}{CiR^3} \approx \dfrac{1.8}{\sqrt{N \cdot SNR_b}}\dfrac{1}{CiR^3} & \text{for} \quad CiR \le 1.2 \\ \dfrac{0.87}{2^b\sqrt{N}} \approx \dfrac{1.1}{\sqrt{N \cdot SNR_b}} & \text{for} \quad CiR > 1.2 \end{cases}. \tag{7}$$

Introduced here, $SNR_b = 1.5 \times 2^{2b}$ is a well-known basic parameter that defines the b-bit A/D converter process dynamics. It is defined as the ratio of the sampled sinusoidal signal power to the power of the quantization noise that is modeled by a random variable with a uniform distribution.

Metrol. Meas. Syst., Vol. XXI (2014), No. 3, pp. 423–432.

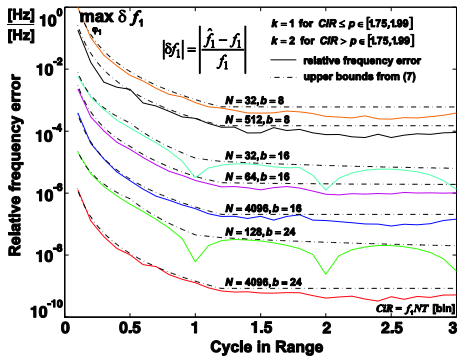

Fig. 6. The frequency estimation error (solid line) and its upper bound (dashed line) using Eqs. (5)-(7) for selected N and b values.

6. Conclusions

The photovoltaic system consists of three main components: the solar panels, inverter and control unit. The quality of the generated signal is influenced by the accuracy of the grid signal frequency estimation.

This paper presents research on the dependence of the accuracy of the developed frequency estimation method [13] on the number of bits b, the A/D converter in the DSP system, the grid signal phase shift relative to the time window, the time window width relative to the grid signal period expressed as the CiR parameter and the number of samples N obtained in the time window. It is shown (Fig. 3) that the largest estimation error occurs when the signal module maximum is in the time window center (for small values of CiR – below 1) or when the signal value is zero in the time window center (for large values of CiR). For these cases (Fig. 4), the equations to estimate the error depending on the CiR value were determined. It is also shown in Tab. 2 that the CiR value should change the k value from 1 to 2 (for most practical cases, the threshold is 1.8). The upper bound of the estimation error is shown in (5)-(7), which demonstrates that the estimation error is the sum of two components: the systematic error, which is inversely proportional to the N^4 value, and the error caused by quantization noise, which is inversely proportional to the square root of the product of the N value for the SNR ratio used for the A/D converter. In practical applications (N=32,...,4096; b=8,..,24), the dominant component of the frequency estimation error is the error caused by the quantization noise. For $CiR > 1.2$, it is approximately 8×10^{-10},..,6×10^{-4}. For $CiR \le 1.2$, it significantly increases when the CiR values decrease and is inversely proportional to CiR^3 (Fig. 6, Eqn. 7).

The results allow for the optimal selection of the number of A/D converter bits in the control unit for the renewable energy system and the estimation of the error level for the grid signal frequency estimation.

References

[1] Rahim, N.A, Selvaraj, J., Solangi, K.H. (2013), Energy policy to promote photovoltaic generation, *Renewable & Sustainable Energy Reviews*, 8, 44–58.

[2] Mamarelis, E., Petrone, G. (2013), An Hybrid Digital-Analog Sliding Mode Controller for Photovoltaic Applications, *IEEE Transactions on Industrial Informatics*, 9(2), 1094–1103.

[3] Thang, T. V., Thao, N., M., Jang.H., Park, J.H. (2014), Analysis and Design of Grid-Connected Photovoltaic Systems With Multiple-Integrated Converters and a Pseudo-DC-Link Inverter, *IEEE Transactions on Industrial Electronics,* 61(7), 3377–3386.

[4] *Characteristics of the utility interface for photovoltaic (pv) systems*, (2002), IEC 61727-2002.

[5] *IEEE recommended practice for utility interface of photovoltaic (PV) systems*, (2000), IEEE Std 929-2000.

[6] *IEEE standard for interconnecting distributed resources with electric power systems*, (2003), IEEE Std 1547-2003.

[7] Selvaraj, J., Rahim, N.A., Krismadinata, C. (2008), Digital PI Current Control for Grid Connected PV Inverter, *3rd IEEE Conference on Industrial Electronics and Applications*, 742–746.

[8] Cha, H., Vu, T., Kim, J. (2009), Design and Control of Proportional-Resonant Controller Based Photovoltaic Power Conditioning System*, IEEE Energy Conversion Congress and Exposition*, 2198–2205.

[9] Ciobotaru, M. (2009), Reliable Grid Condition Detection and Control of Single-Phase Distributed Power, Faculty of Engineering, Aalborg University.

[10] Zygarlicki, J., Mroczka, J. (2012), Variable-frequency prony method in the analysis of electrical power quality, *Metrology and Measurement Systems*, 19(4), 659–672.

[11] Borkowski, J., Mroczka, J. (2010), LIDFT method with classic data window and zero padding in multifrequency signal analysis, *Measurement*, 43, 1595–1602.

[12] Borkowski, J., Mroczka, J. (2002), Metrological analysis of the LIDFT method, *IEEE Transactions on Intrumentation and Measurement*, 51, 66–71.

[13] Borkowski, J., Kania, D., Mroczka J. (2014), Interpolated DFT-based Fast and Accurate Frequency Estimation for the Control of Power, *IEEE Transactions on Industrial Electronics*, DOI:10.1109/TIE.2014.2316225.

[14] Femia, N., Petrone, G., Spagnuolo, G., Vitelli M. (2013), *Maximum Energy Harvesting in Photovoltaic Systems,* Boca Raton: CRC Press, 129–136.

[15] Widrow, B., Kollar, I. (2008), Quantization Noise: Roundoff Error in Digital Computation, Signal Processing, Control, and Communications, New York: Cambridge University Press.

[16] Norsworthy, S., Schreier R., Temes G. (1997), Delta-Sigma Data Converters, Theory, Design and Simulation, New Jersey: Wiley&Sons.

[17] Geng, H., Sun, J., Xiao, S., Yang, G. (2013), Modeling and Implementation of an All Digital Phase-Locked-Loop for Grid-Voltage Phase Detection, *IEEE Transactions on Industrial Informatics*, 9(2), 772–780.

[18] Najafi, E., Yatim, A.H.M. (2012), Design and Implementation of a New Multilevel Inverter Topology, *IEEE Transactions on Industrial Electronics,* 59(11), 4148–4154.

[19] Attaianese, C., Di Monaco, M., Tomasso, G. (2013), High Performance Digital Hysteresis Control for Single Source Cascaded Inverters, *IEEE Transactions on Industrial Informatics*, 9(2), 620–629.

[20] Zeng, Z., Yang, H., Zhao, R., Cheng, C. (2013), Topologies and control strategies of multi-functional grid-connected inverters for power quality enhancement: A comprehensive review, *Renewable & Sustainable Energy Reviews*, 24, 223–270.

[21] Avelar, H.J., Parreira, W.A., Vieira, J.B., de Freitas, L.C.G., Coelho, E.A.A. (2012), A State Equation Model of a Single-Phase Grid-Connected Inverter Using a Droop Control Scheme With Extra Phase Shift Control Action, *IEEE Transactions on Industrial Electronics*, 59(3), 1527–1537.

[22] Yousefpoor, N., Fathi, S.H., Farokhnia, N., Abyaneh, H.A. (2012), THD Minimization Applied Directly on the Line-to-Line Voltage of Multilevel Inverters, *IEEE Transactions on Industrial Electronics*, 59(1), 373–380.

[23] Vazquez, S., Sanchez, J.A., Reyes, M. R., Leon, J.I. (2014), Adaptive Vectorial Filter for Grid Synchronization of Power Converters Under Unbalanced and/or Distorted Grid Conditions, *IEEE Transactions on Industrial Electronics*, 61(3), 1355–1367.

[24] Etemadi, A., Iravani, R. (2013), Overcurrent and Overload Protection of Directly Voltage-Controlled Distributed Resources in a Microgrid, *IEEE Transactions on Industrial Electronics*, 60(12).

[25] Francesco, De M., Marco, L., Antonio, D.A., Alberto, P. (2006), Overview of antiislanding algorithms for PV systems. Part I: Passive methods, *12th International Power Electronics and Motion Control Conference (EPE-PEMC),* 1878–1883.